Article:

Harman-Thomas, J.M. orcid.org/0000-0003-3287-6050, Ingham, D.B., Hughes, K.J. et al. (1 more author) (2023) Role of methyldioxy radical chemistry in high-pressure methane combustion in CO2. International Journal of Chemical Kinetics, 55 (10). pp. 629-641. ISSN 0538-8066

https://doi.org/10.1002/kin.21672

Received: 23 December 2022 | Revised: 28 May 2023 | Accepted: 28 May 2023

DOI: 10.1002/kin.21672

INTERNATIONAL JOURNAL OF CHEMICAL KINETICS WILEY

RESEARCH ARTICLE

Role of methyldioxy radical chemistry in high-pressure methane combustion in CO_2

James M. Harman-Thomas | **Derek B. Ingham** | **Kevin J. Hughes** | **Mohamed Pourkashanian**

Department of Mechanical Engineering, Translational Energy Research Centre, The University of Sheffield, Sheffield, UK

Correspondence
Kevin J. Hughes, Department of Mechanical Engineering, Translational Energy Research Centre, The University of Sheffield, Sheffield, UK.
Email: k.j.hughes@sheffield.ac.uk

Funding information
Engineering and Physical Sciences Research Council; International Flame Research Foundation

Abstract

The combustion chambers of direct-fired supercritical CO_2 power plants operate at pressures of approximately 300 bar and CO_2 dilutions of up to 96%. The rate coefficients used in existing chemical kinetic mechanisms are validated for much lower pressures and much smaller concentrations of CO_2. Recently, the UoS sCO_2 1.0 and UoS sCO_2 2.0 mechanisms have been developed to better predict ignition delay time (IDT) data from shock tube studies at pressures from 1 to 260 bar in various CO_2-containing bath gas compositions. The chemistry of the methyldioxy radical (CH_3O_2) has been identified as an essential combustion intermediate for methane combustion above 100 bar, where mechanisms missing this species begin to vastly overpredict the IDT. The current literature available on CH_3O_2 is very limited and often concerned with atmospheric chemistry and low-pressure, low-temperature combustion. This means that the rate coefficients used in UoS sCO_2 2.0 are commonly determined at sub-atmospheric pressures and temperatures below 1000 K with some rate coefficients being over 30 years old. In this work, the rate coefficients of new potential CH_3O_2 reactions are added to the current mechanism to create UoS sCO_2 2.1 It is shown that the influence of CH_3O_2 on the IDT is greatest at high pressures and low temperatures. It has also been demonstrated that CO_2 has very little effect on the chemistry of CH_3O_2 at 300 bar meaning that CH_3O_2 rate coefficients can be determined in other bath gases, reducing the impact of non-ideal effects such as bifurcation when studying in a CO_2 bath gas. The updated UoS sCO_2 2.1 mechanism is then compared to high-pressure IDT data and the most important reactions which require reinvestigation have been identified as the essential next steps in understanding high-pressure methane combustion.

KEYWORDS

CH_3O_2, chemical kinetics, methane, supercritical CO_2

1 | INTRODUCTION

In recent years, the energy trilemma has become increasingly challenging on all three fronts. On the fuel security and equity fronts, the recent war in Ukraine has interrupted the supply of Russian gas to European countries and inflated oil and gas prices, forcing major European countries to find alternate suppliers, namely the United States and the Middle East.[1,2] Additionally, on the environmental security front, the 2019 "The Truth Behind the Climate Pledges" report found that 75% of the 184 report countries that signed up to the Paris Agreement had taken insufficient action to curb global temperature rises, with some still increasing their emissions.[3] Bringing together all these challenges identifies a need for energy technologies that provide for emissions-free energy generation from the combustion of fossil fuels.

Direct-fired supercritical CO_2 (sCO_2) power cycles such as the Allam-Fetvedt cycle[4] and the Supercritical Transformational Electric Power (STEP) project[5] have been proposed as methods of emissions-free power generation from fossil fuels. The Allam-Fetvedt cycle, the most developed of the two, burns a mixture of methane and oxygen in a 96% CO_2 dilution at pressures up to 300 bar.[4] Due to the combustion taking place in pure oxygen and CO_2, the only major products are CO_2 and water (H_2O), which can be easily separated to create a high-purity stream of sCO_2, ideal for transportation and subsequent storage or utilization. This means that Allam-Fetvedt cycle power plants have 100% carbon capture, at a price competitive with existing fossil-fueled power plants without carbon capture and storage. This is due to the greater power density of sCO_2 compared to traditional working fluids, and the high pressure reduces the overall plant footprint.[4] The deployment of the Allam-Fetvedt cycle worldwide has begun with the recent announcement of two new power plants in development in the United States.[6] and one in the United Kingdom.[7]

Most chemical kinetic combustion mechanisms have been developed using experimental data recorded at pressures and CO_2 dilutions much smaller than those of the Allam-Fetvedt cycle.[8] Recently, Harman-Thomas et al.[9] studied the performance of four existing chemical kinetic mechanisms for modeling ignition delay time (IDT) of 52 datasets of methane, hydrogen, and syngas combustion at a range of equivalence ratios, pressures, temperatures, and fuel ratios in various concentrations of CO_2. From this work and Harman-Thomas et al.,[10,11] the University of Sheffield (UoS) sCO_2 2.0 mechanism was created and verified for methane, hydrogen, and syngas IDTs. Karimi et al.[12] first noted the importance of CH_3O_2 chemistry in CO_2 at 100 bar and 200 bar and this chemistry was subsequently found to the essential to the creation of UoS sCO_2 1.0. The rate coefficients for the reactions of CH_3O_2 are often poorly understood with rate coefficients from outdated literature sources that have large uncertainty values, often not having been measured directly, and are based on estimations of similar reactions.

2 | METHYLDIOXY RADICAL CHEMISTRY

A literature review of CH_3O_2 chemistry will bring up research focusing on its relevance to the oxidation of atmospheric hydrocarbons.[13] In atmospheric chemistry, CH_3O_2 is an important intermediate in the low-pressure, low-temperature oxidation of hydrocarbons, predominantly reacting with NO, HO_2, and OH.[14] Similarly, CH_3O_2 chemistry has also been discussed in its relevance to low-temperature combustion where the third-body reaction to form CH_3O_2 via Reaction 1 is favored, due to the complexes increased stability at low temperatures.[15,16] This means that most rate coefficients available for CH_3O_2 chemistry currently used in chemical kinetic mechanisms are based on experimental data or theoretical calculations for temperatures and pressures well below that of the Allam-Fetvedt cycle. The importance of CH_3O_2 chemistry to the combustion of the Allam-Fetvedt cycle has been discussed by Karimi et al.[12] and Harman-Thomas et al.[9] and the role of CH_3O_2 in the high-pressure oxidation of methane in Hashemi et al.[17] where it was noted that CH_3O_2 was pivotal for simulating CO_2 formation. It was observed that the USC II[18] and GRI 3.0[19] chemical kinetic mechanisms overpredicted IDTs above 100 bar due to their lack of CH_3O_2 chemistry. The subsequent addition of the CH_3O_2 and CH_3O_2H species and 14 of their reactions significantly improve these mechanisms' ability to model high-pressure methane IDTs.[9] Similarly, Shao et al.[20] found that FFCM-1,[21] a mechanism which also does not contain CH_3O_2 chemistry, also showed poor agreement with the high-pressure methane IDTs. The present study seeks to improve upon UoS sCO_2 2.0 by updating the mechanism with the most accurate rate coefficients from more recent theoretical, experimental, and mechanistic studies as listed in Table 1.

In the present study, the CH_3O_2 chemistry in UoS sCO_2 2.0 was expanded through the addition of new reactions CH_3O_2, updating rate coefficients, and the addition of CH_2O_2H. The importance of the addition of each of these reactions is then discussed and the mechanism created from the rate coefficients listed in Table 1 is denoted as UoS sCO_2 2.1.

TABLE 1 Rate coefficients of CH_3O_2 reactions in the UoS sCO_2 2.1 mechanism.

Reaction	A (cm^3 mol s)	*n*	Ea (cal/mol)	Ref.
Reaction 1 (DUP) $CH_3 + O_2\ (+M) \rightleftharpoons CH_3O_2\ (+M)$[a]	5.0×10^{22} 5.0×10^{22}	−3.85 −3.85	2000 2000	17
Reaction 2 $CH_4 + CH_3O_2 \rightleftharpoons CH_3 + CH_3O_2H$	1.81×10^{11}	0.00	18,480	22
Reaction 3 $CH_3O_2 + O \rightleftharpoons CH_3O + O_2$	2.9×10^{10}	1.00	−724	17
Reaction 4 $CH_3O_2 + H \rightleftharpoons CH_3O + OH$	9.6×10^{13}	0.00	0	23
Reaction 5 $CH_3O_2 + OH \rightleftharpoons CH_3OH + O_2$	1.7×10^{14}	0.00	0	24
Reaction 6 $CH_3O_2 + HO_2 \rightleftharpoons CH_3O_2H + O_2$	2.47×10^{11}	0.00	−1570	25
Reaction 7 $CH_3O_2H + HO_2 \rightleftharpoons CH_3O_2 + H_2O_2$	4.01×104	2.50	10,206	26
Reaction 8 $CH_3O_2 + CH_3 \rightleftharpoons CH_3O + CH_3O$	5.08×10^{12}	0.00	−1411	27
Reaction 9 $CH_3O_2 + CH_3O_2 \rightleftharpoons CH_2O + CH_3OH + O_2$	2.0×10^{11}	−0.55	−1600	28
Reaction 10 (DUP) $CH_3O_2 + CH_3O_2 \rightleftharpoons O_2 + CH_3O + CH_3O$	1.1×10^{18} 7.0×10^{10}	−2.4 0	1800 8000	28
Reaction 11 $H_2 + CH_3O_2 \rightleftharpoons H + CH_3O_2H$	1.5×10^{15}	0.00	26,030	29
Reaction 12 $CH_3OH + CH_3O_2 \rightleftharpoons CH_2OH + CH_3O_2H$	2.06×10^{-9}	6.20	7128	22
Reaction 13 $CH_2O + CH_3O_2 \rightleftharpoons HCO + CH_3O_2H$	1.981×10^{9}	1.111	12,499.5	30
Reaction 14 $CH_3O_2H\ (+M) \rightleftharpoons CH_3O + OH\ (+M)$[a]	4.1×10^{19}	−1.153	44,226	31
Reaction 15 $C_2H_6 + CH_3O_2 \rightleftharpoons C_2H_5 + CH_3O_2\ H$	4.04×10^{1}	3.55	16,900	32
Reaction 16 $C_2H_4 + CH_3O_2 \rightleftharpoons C_2H_3 + CH_3O_2H$	3.83×10^{3}	3.06	20,799	33,34
Reaction 17 $CO + CH_3O_2 \rightleftharpoons CH_3O + CO_2$	4.22×10^{6}	0.00	0	35
Reaction 18 $CH_3O_2 + H \rightleftharpoons CH_4 + O_2$	7.05×10^{12}	1.02	16,599	36
Reaction 19 $CH_3O_2 + OH \rightleftharpoons CH_3O + HO_2$	4.54×10^{13}	−0.22	−363	37
Reaction 20 $CH_3O_2 + HO_2 \rightleftharpoons CH_2O + H_2O + O_2$	9.64×10^{8}	0.00	3437	38
Reaction 21 $CH_3OH + CH_3O_2 \rightleftharpoons CH_3O + CH_3O_2H$	7.937×10^{8}	4.71	13,560	39
Reaction 22 $CH_3O_2H + H \rightleftharpoons CH_2O_2H + H_2$	5.4×10^{10}	0	1860	40
Reaction 23 $CH_3O_2H + H \rightleftharpoons CH_3O + H_2O$	1.2×10^{10}	0	1860	40
Reaction 24 $CH_3O_2H + O \rightleftharpoons CH_2O_2H + OH$	1.6×10^{13}	0	4750	28
Reaction 25 $CH_3O_2H + O \rightleftharpoons CH_3O_2 + OH$	8.7×10^{12}	0	4750	28

(Continues)

TABLE 1 (Continued)

Reaction	A (cm^3 mol s)	*n*	Ea (cal/mol)	Ref.
Reaction 26 $CH_3O_2H + OH \rightleftharpoons CH_3O_2 + H_2O$	1.1×10^{12}	0	−437	[28]
Reaction 27 $CH_3O_2H + OH \rightleftharpoons CH_2O_2H + H_2O$	7.2×10^{11}	0	−258	[28]
Reaction 28 $CH_2O_2H\ (+M) \rightleftharpoons CH_2O + OH\ (+M)$[a]	2.4×10^{12}	−0.925	1567	[41]

[a] Pressure dependence.

Preliminary reaction pathway analysis (RPA) revealed ethane (C_2H_6) formation via the recombination of methyl radicals (CH_3) in Reaction 29. Similarly, ethane (C_2H_4) and acetaldehyde (CH_3CHO) are stable intermediates in methane combustion, so these reactions may be influential in the CH_3O_2 chemistry. Reaction 17 was added as Harman-Thomas et al.[11] showed that CO formation via the reverse of Reaction 30 was appreciable when using a CO_2 bath gas, due to the large concentration of CO_2 making this reaction more favorable. This coupled with CO being a stable intermediate of methane combustion means that even though this rate coefficient is small, at large concentrations of CO it may be important, especially at the highest values of uncertainty. Bogdanchikov et al.[36] showed that the reverse of Reaction 18 was negligible compared to the accepted Reaction 31 at normal combustion conditions due to the large activation energy. The reaction was included because it may become more important at higher pressures due to the larger mole fraction of CH_3O_2 at 300 bar relative to typical combustion pressures. Zhao et al.[39] studied the two competing reactions Reaction 12 and Reaction 21 at 1 atm from 300–1500 K and found that Reaction 21 became increasingly important as the temperature increased, becoming the dominant pathway at 1500 K.

$$CH_3 + CH_3\,(+M) = C_2H_6\,(+M) \qquad \text{(Reaction 29)}$$

$$CO + OH = CO_2 + H \qquad \text{(Reaction 30)}$$

$$CH_4 + O_2 = CH_3 + HO_2 \qquad \text{(Reaction 31)}$$

3 | MODELLING PROCEDURE

The modeling work in this work was performed using ANSYS Chemkin-Pro 2019 R3. To focus on the chemical kinetics a closed homogeneous batch reactor was used with the "constrain the volume and solve energy equation" problem type. The base conditions were set to resemble those of the Allam-Fetvedt cycle to focus on the role of CH_3O_2 at large pressures. A pressure of 300 bar and a CO_2 dilution of 96% was used, while the temperature was assumed to be 1100 K.[42] As the exact fuel-air concentrations have not been published, a stoichiometric ($\phi = 1.0$) methane/oxygen mixture was used in a 96% dilution of CO_2. The UoS sCO_2 2.1 mechanism was used to evaluate the need for the updated rate coefficients as well as including the important base Chemistry of UoS sCO_2 2.0, which was shown to better model high-pressure IDTs of methane in a CO_2 bath gas.[12,20]

The chemistry of CH_3O_2 was investigated using sensitivity analysis, reaction pathway analysis and rate of production (ROP) analysis. Combining these analyses shows the contribution of CH_3O_2 chemistry to the combustion of methane. The newly created UoS sCO_2 2.1 mechanism was then compared to existing high-pressure literature IDT data to see how the changes made in the mechanism affected the simulations. Furthermore, the role of CO_2 as a bath gas was investigated in CH_3O_2 chemistry, by repeating the experimental run with a 96% N_2 and Ar bath gas. The IDT was determined as the time of maximum gradient in the temperature profile of the reaction.

4 | ROLE OF CH_3O_2 CHEMISTRY AT 300 BAR

Following the modelling procedure outlined, the chemistry of CH_3O_2 was modeled at conditions relevant to the Allam-Fetvedt cycle. Figure 1A shows the mole fraction of nine selected radical species over the first 5 ms of the reaction including CH_3O_2 and CH_3O_2H with Figure 1B focuses in on the three species of smallest concentration. The mole fraction of CH_3O_2 in Figure 1 is comparable to CH_3 under these conditions, 100% of methane will form CH_3, and as the mole fraction of CH_3O_2 exceeds this. This suggests that the species has a reactivity smaller than CH_3, allowing an appreciable concentration to build up. Furthermore, the CH_3O_2 mole fraction is greatest at the start of the reaction, before the ignition, suggesting that it plays a key role in the onset of ignition, explaining its importance to

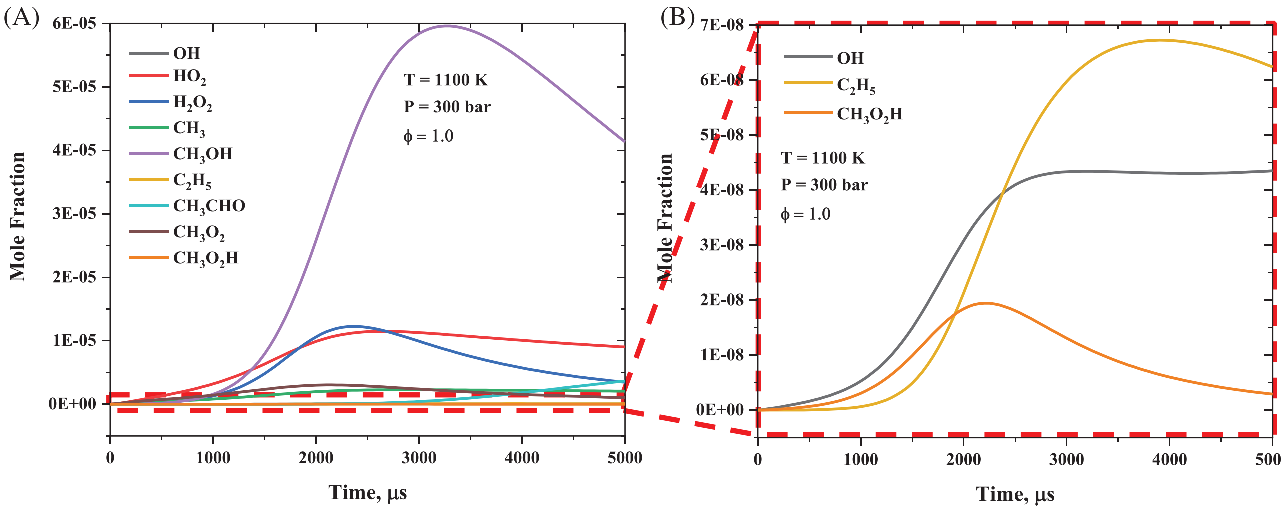

FIGURE 1 Mole fraction of selected radical and combustion intermediates at 1100 K and 300 bar (CH_4:O_2:CO_2 = 1.333:2.667:96) simulated by UoS sCO_2 2.1.

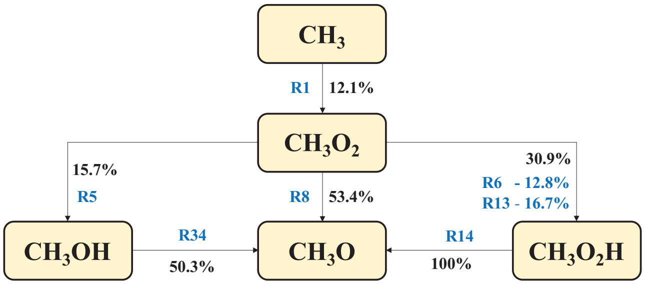

FIGURE 2 CH_3O_2 reaction pathway at the point of ignition at 1100 K and 300 bar (CH_4:O_2:CO_2 = 1.333:2.667:96) simulated by UoS sCO_2 2.1.

high-pressure methane IDTs. However, the mole fraction of CH_3O_2H is much smaller and more closely resembles that of OH at the point of ignition despite Figure 2 showing that 30.9% of CH_3O_2 goes on to form CH_3O_2H. This suggests that CH_3O_2H dissociates almost instantaneously via Reaction 14 to form CH_3O and OH under these conditions. Interestingly, Figure 1 shows that the OH concentration continues to increase after the ignition event due to the slower dissociation of H_2O_2. CH_3O an important product from the reactions of CH_3O_2 is omitted from Figure 1 as the species reacted meaning a meaningful concentration is not achieved.

Figure 2 shows the key reactions and intermediates in the CH_3O_2 reaction pathway. The formation of CH_3O_2 via Reaction 1 competes with Reaction 32 and Reaction 33. At 300 bar, Reaction 1 and Reaction 33 are the major reaction pathways of the $CH_3 + O_2$ reaction. These two reactions collectively account for almost 25.5% of CH_3 consumption. At 30 bar, Reaction 1 is not a viable reaction path and therefore the CH_3O_2 reaction pathway is negligible as almost all $CH_3 + O_2$ proceeds via Reaction 33. It must also be noted that Karimi et al.[12] highlighted the greater importance of Reaction 2 in their datasets, most likely due to the greater fuel concentrations and thus increased methane concentration.

$$CH_3 + O_2 \rightleftharpoons O + CH_3O \qquad \text{(Reaction 32)}$$

$$CH_3 + O_2 \rightleftharpoons OH + CH_2O \qquad \text{(Reaction 33)}$$

As seen in Figure 2, 84.3% of CH_3O_2 formed reacts to form CH_3O, either directly through Reaction 8 or via CH_3O_2H. The remaining CH_3O_2 reacts with OH in Reaction 5 to form CH_3OH, and approximately half of CH_3OH subsequently reacts to form CH_3O under these conditions. As shown in Figure 3 the majority of CH_3O reacts to form CH_2O either via dissociation in Reaction 35 or by reacting with O_2 in Reaction 35. Furthermore, despite Figure 3 showing that the majority of CH_3O is formed through Reaction 36, the next three biggest producers of CH_3O are via the CH_3O_2 reaction pathway and cumulatively account for approximately one-third of the total production.

$$CH_3O\,(+M) \rightleftharpoons CH_2O + H\,(+M) \qquad \text{(Reaction 34)}$$

$$CH_3O + O_2 \rightleftharpoons CH_2O + HO_2 \qquad \text{(Reaction 35)}$$

$$CH_3 + HO_2 = CH_3O + OH \qquad \text{(Reaction 36)}$$

Figure 4 shows the percentage of CH_3O production (dashed) and loss (solid) from 1000–1500 K across the completion reaction. Across the full temperature range, Reactions 34 and 35 remain similar in terms of CH_3O loss

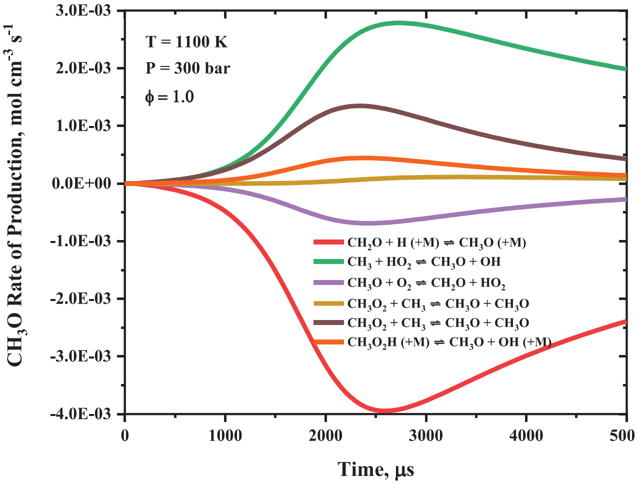

FIGURE 3 Rate of CH_3O production at 1100 K and 300 bar simulated by UoS sCO_2 2.1.

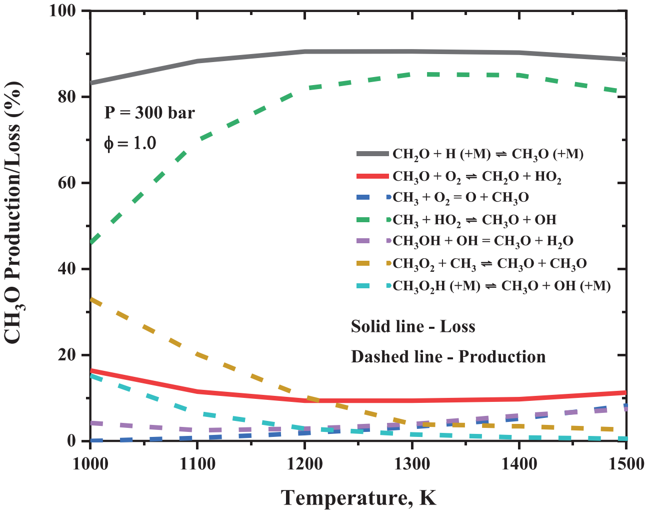

FIGURE 4 Percentage of CH_3O production (dashed) and loss (solid) simulated by UoS sCO_2 2.1.

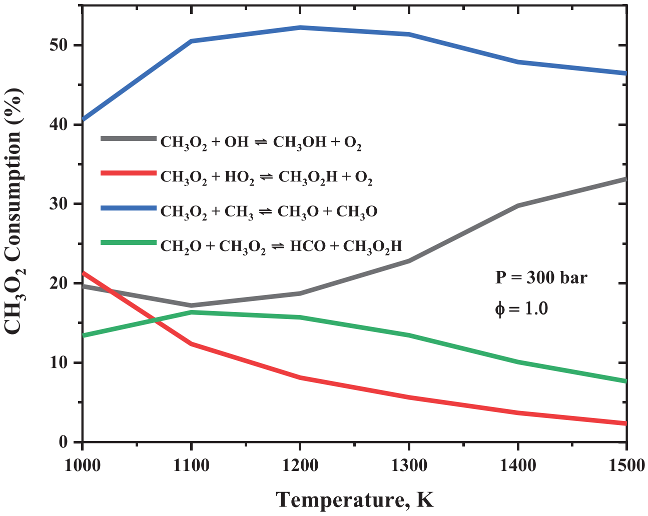

FIGURE 5 Effect of temperature on the consumption of CH_3O_2 and the maximum net production rate of CH_3O_2 simulated by UoS sCO_2 2.1.

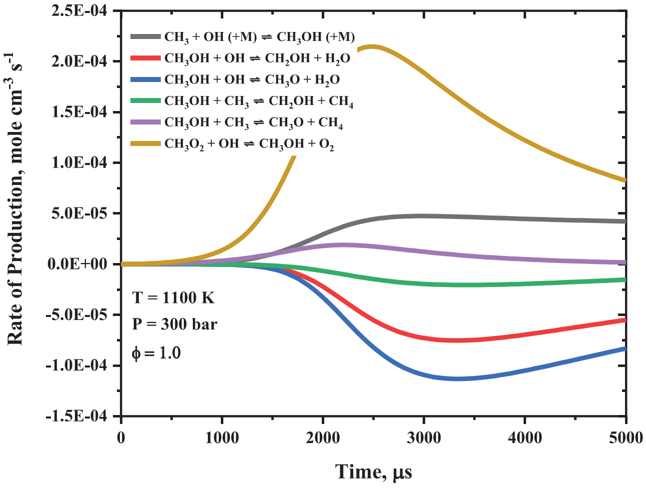

FIGURE 6 CH_3OH rate of production at 1100 K and 300 bar simulated by UoS sCO_2 2.1.

at approximately 85% and 15% respectively. Reaction 36 is the prominent route of CH_3O formation at 1000 K and becomes increasingly important as the temperature increases. The CH_3O_2 reaction pathway contributes to approximately 50% CH_3O formation at 1000 K via Reactions 8 and 14 but this contribution is negligible at 1500 K, indicating a strong influence of temperature on CH_3O_2 formation.

Figure 5 shows the percentage consumption of CH_3O_2 at 300 bar between 1000 and 1500 K to see the influence of temperature on the reactivity since many of the rate coefficients listed in Table 1 have large temperature coefficients. Of the four most important reactions, Reaction 8 contributes to almost 45% of CH_3O_2 consumption during the reaction. Reactions 6 and 13 become decreasingly important with temperature whilst Reaction 5 increases to compensate for this change. All other reactions listed in Table 1 are negligible under these conditions but could become more important at different pressure and different fuel/oxidizer combinations.

The other reactant, CH_3OH, must be considered as Figure 2 shows that 15.7% of CH_3O_2 goes on to form CH_3OH via Reaction 5. Figure 6 shows the rate of CH_3OH production/loss at 1100 K and 300 bar. CH_3OH is formed primarily through Reaction 5 with Reactions 37 and 38 playing a much smaller role. CH_3OH is then consumed by reactions with OH via Reactions 39 and 40. Therefore, under these conditions, it can be considered that CH_3O_2 formation dominates CH_3OH formation which subsequently reacts with OH to form H_2O and CH_3O or CH_2OH.

However, it is important to note that there an alternate rate coefficient for Reaction 5 from Zhang and Huang[37] would significantly deemphasize the role of CH_3O_2 on CH_3OH formation. Both the rate coefficients of Bossolasco et al.[24] and Zhang and Huang[37] are validated for atmospheric chemistry and thus extrapolated well-beyond the conditions they were determined for when simulating the Allam-Fetvedt cycle. Bossolasco et al.[24] was selected in this work due to it being determined using experimentally as well as being previously validated for a high-pressure methane combustion mechanism[17] and the negative effect Zhang and Huang[37] had on simulating the experimental data of Karimi et al.[12] However, given the large difference in the importance of CH_3O_2 in CH_3OH formation at high-pressures, it is essential that this rate coefficient is investigated under these conditions as a matter of research priority.

$$CH_3 + OH\,(+M) \rightleftharpoons CH_3OH\,(+M) \qquad \text{(Reaction 37)}$$

$$CH_3OH + CH_3 \rightleftharpoons CH_3O + CH_4 \qquad \text{(Reaction 38)}$$

$$CH_3OH + OH = CH_2OH + H_2O \qquad \text{(Reaction 39)}$$

$$CH_3OH + OH = CH_3O + H_2O \qquad \text{(Reaction 40)}$$

4.1 | Branching of $CH_3 + O_2$ reactions

The formation of CH_3O_2 is completely due to the reaction of CH_3 and O_2 which makes the branching ratio of these reactions extremely important to the overall chemistry. As discussed, the rate of Reaction 32 is negligible at 300 bar. Therefore, only the rates of Reaction 1 and Reaction 33 need to be considered. Figure 7 shows the ratio of the net reaction rates Reaction 33/Reaction 1 at pressures ranging from 1 to 300 bar across the first 5000 ms of the reaction. As the pressure increases, the ratio decreases significantly from Reaction 1 which is negligible at 1 bar but becomes much more important at 100 bar and even the dominant reaction after ignition at 300 bar.

5 | EFFECT OF TEMPERATURE AND PRESSURE ON IGNITION DELAY TIME

It was first noted by Karimi et al.[12] that CH_3O_2 had an important influence on the IDT at pressures above 100 bar. It is also well-established that CH_3O_2 is an important intermediate in low-temperature combustion.[43] The influence of CH_3O_2 on the IDT was investigated over a pressure and temperature range of 1–300 bar and 1000–2000 K, respectively. The IDT was determined as the time of the maximum gradient on the dT/dt curve. The IDT difference (%) was determined by finding the IDT using the UoS sCO_2 2.1 mechanism and a modified version of the UoS sCO_2 2.1 mechanism which had all CH_3O_2 chemistry removed. The percentage difference was then determined which is shown in a contour plot in Figure 8. The importance of CH_3O_2 to the IDT is greatest at 300 bar and 1000 K, which is to be expected based on previous research. The difference between the simulated IDTs here exceeds 140%, with the mechanism not containing CH_3O_2 predicting the slower IDT. Furthermore, at only 50 bar and 1000 K removing the CH_3O_2 chemistry leads to an increase in IDT by

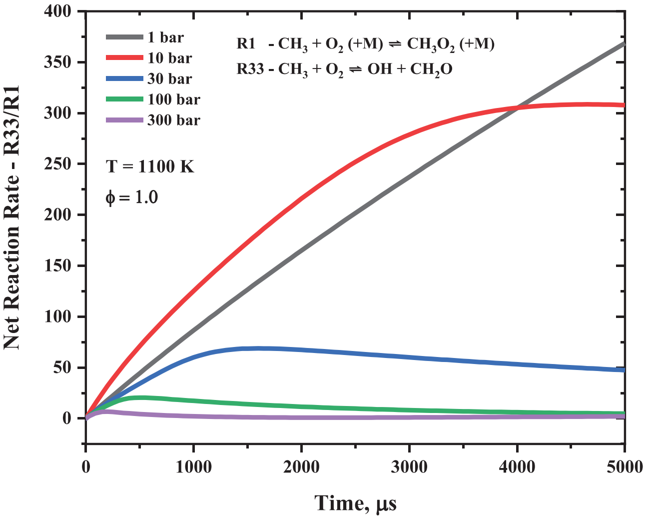

FIGURE 7 The ratio of the Net Reaction Rate of Reaction 33/Reaction 1 at pressures from 1 to 300 bar.

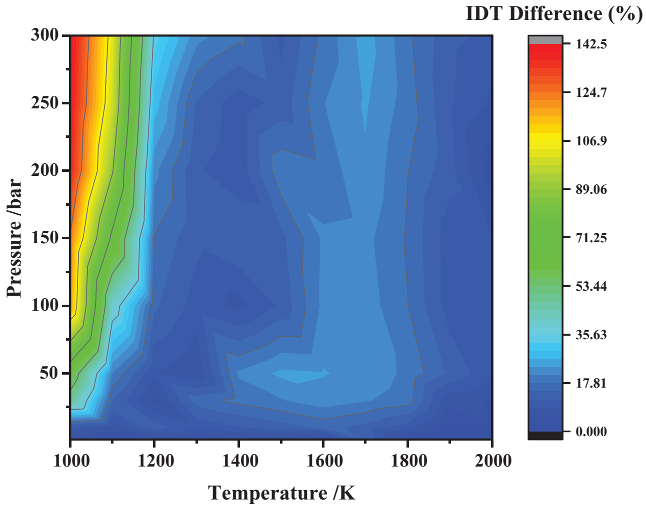

FIGURE 8 Contour plot of the difference in ignition delay time at pressures from 1–300 bar and 1000–2000 K with CH_3O_2 chemistry included in the UoS sCO_2 2.1 mechanism.

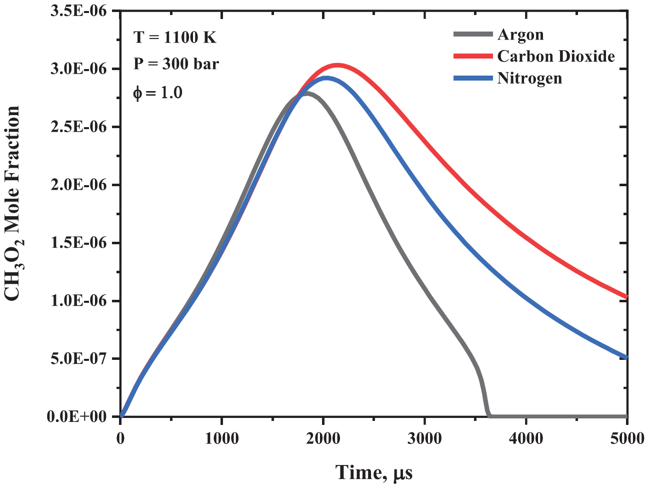

FIGURE 9 CH_3O_2 mole fraction for stoichiometric CH_4 combustion in 96% carbon dioxide, nitrogen, and argon diluent at 1100 K and 300 bar.

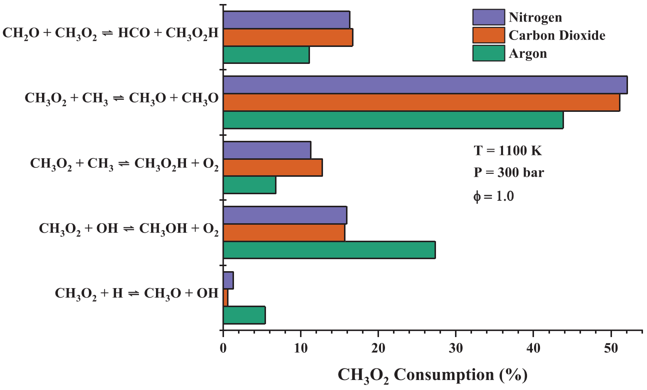

FIGURE 10 Percentage of CH_3O_2 consumption for the five critical removal reactions for three different bath gas (carbon dioxide, nitrogen, and argon) at 1100 K and 300 bar.

approximately 50%. This shows a significant role of CH_3O_2 at even lower pressures than discussed in Harman-Thomas et al.,[9] highlights the importance of using a mechanism which contains CH_3O_2 chemistry to model methane combustion in CO_2 at pressures above 50 bar. Mechanisms such as FFCM-1,[21] USC II[18] and GRI 3.0[19] should be restricted to pressures below 50 bar when studying combustion at less than 1200 K. It should also be noted the deep blue may still indicate a pressure difference of almost 20%. Considering the experimental error in shock tubes typically varies from 15% to 25%,[10,11] this could still lead to large errors in chemical kinetic models. Furthermore, there is also a need to populate the current gap in methane IDT data which exists between 40 and 80 bar, to compare the effect of CH_3O_2 on the IDT across this range where it is predicted to become an important factor. Utilizing rapid compression machines (RCMs) would allow the study of high-pressure combustion of CO_2 at much lower temperatures in shock tubes due to the longer achievable test times.

6 | EFFECT OF CO_2 ON CH_3O_2 CHEMISTRY

As autoignition is rarely studied at pressures greater than 100 bar, the importance of CH_3O_2 in the combustion of methane in Argon, N_2 and CO_2 has only been discussed briefly in existing literature.[12,17,44,45] Figure 9 shows the mole fraction of CH_3O_2 for stoichiometric methane combustion at 1100 K and 300 bar in 96% CO_2, N_2, and Argon. Despite the different temperatures achieved, which affect the time of maximum CH_3O_2 mole fraction, the actual maximum mole fraction is consistent between the three gases. As CO_2 is a more efficient absorber of heat than nitrogen, and by extension argon, it absorbs more heat from the reaction and the maximum temperature achieved is less, meaning that slightly more CH_3O_2 is formed as recombination reactions are favored at lower temperatures.

To investigate the influence of CO_2 on the actual chemistry of CH_3O_2 the ROP of CH_3O_2 was explored for the three different gases. As all CH_3O_2 is formed through Reaction 1, and the CH_3O_2 mole fractions are similar, the rate of production is similar for all three bath gases. Figure 10 shows the percentage of CH_3O_2 consumption for the five key reactions. As shown, the chemistry of CH_3O_2 consumption is largely unvaried between CO_2 and N_2. For Ar, the chemistry is slightly different, the most significant change being the greater importance of Reactions 4 and 5 due to the greater temperature achieved due to Ar absorbing the heat of combustion less efficiently. The similarity of the CH_3O_2 chemistry in the different bath gases is an essential observation for two reasons. First, the importance of CH_3O_2 to high-pressure combustion expands beyond the application of direct-fired supercritical CO_2 power cycles. Other applications such as the Space-X Raptor engine which operates using a methane fuel in air at over 300 bar,[46] will also be heavily reliant on CH_3O_2 chemistry and need to have accurate rate coefficients for these reactions to ensure accurate modelling of their combustion. Second, experimental techniques for the high-pressure investigation of CO_2, such as shock tubes, are often susceptible to non-ideal effects such as bifurcation[10,47] which reduces the available test time, increases the uncertainty, and complicates the analysis. Therefore, by understanding that CH_3O_2 chemistry is independent of bath gas, any future experimental work can be performed using argon, simplifying the analysis, and reducing the experimental error, if CO_2 would not have a chemical effect on any of the reactions, except for Reaction 1. It is important to consider however that the rate coefficient used for Reaction 1 has no third-body efficiencies for different gases as the rate coefficient uses a PLOG system to determine the effect of pressure on the reaction.

7 | COMPARISON TO EXPERIMENTAL DATA

The original UoS sCO_2 2.1 mechanism was developed based on three IDT datasets recorded at pressures over 200 bar from Karimi et al.[12] and Shao et al.[20] The mechanism originally showed a good agreement with the data over this pressure range. Figure 11 of NUIGMech1.1, DTU,[48] UoS sCO_2 1.0 and UoS sCO_2 2.1. Interestingly, the updating of the CH_3O_2 rate coefficients in UoS sCO_2 2.1 to those most recently published has slightly worsened the mechanism performance, although b) and Figure 11C) both fall within experimental error. One further improvement required is that Reactions 6 and 8 which were identified as important in Figure 2 are from outdated literature sources and have not been studied more recently to allow these rate coefficients to be updated. Especially given Reaction 8 is responsible for 50% of CH_3O_2 consumption this should be reinvestigated as a research priority. The slight discrepancy from the experimental data could be due to the difference in the chemical kinetic mechanisms used outside of the CH_3O_2 chemistry. However, the significant difference in UoS sCO_2 1.0 and 2.1 shows that these rate coefficients do have a large influence on IDT under these conditions.

8 | RECOMMENDATIONS FOR FUTURE RESEARCH

This present study expands upon the work done by Harman-Thomas et al.[9] and Karimi et al.[12] further divulges the importance of the chemistry of CH_3O_2 to high-pressure combustion in CO_2. New investigations into the important rate coefficients are required for the most important reactions introduced in this work using experimental and theoretical investigations.

8.1 | Important rate coefficients

Previous research into the rate coefficients of the reactions of CH_3O_2 has been performed using high-pressure flow reactors and a pump, probe technique to monitor CH_3O_2 radicals at 210, 224,[49] and 240 nm.[50] The most important reactions of the CH_3O_2 reaction pathway have been discussed in this work and some should be revisited using modern experimental techniques as many rate coefficients currently utilized are based on limited experimental data and are almost 40 years old. As combustion at high pressures is so pertinent to modern applications, assuming full trust in these outdated rate coefficients at conditions well

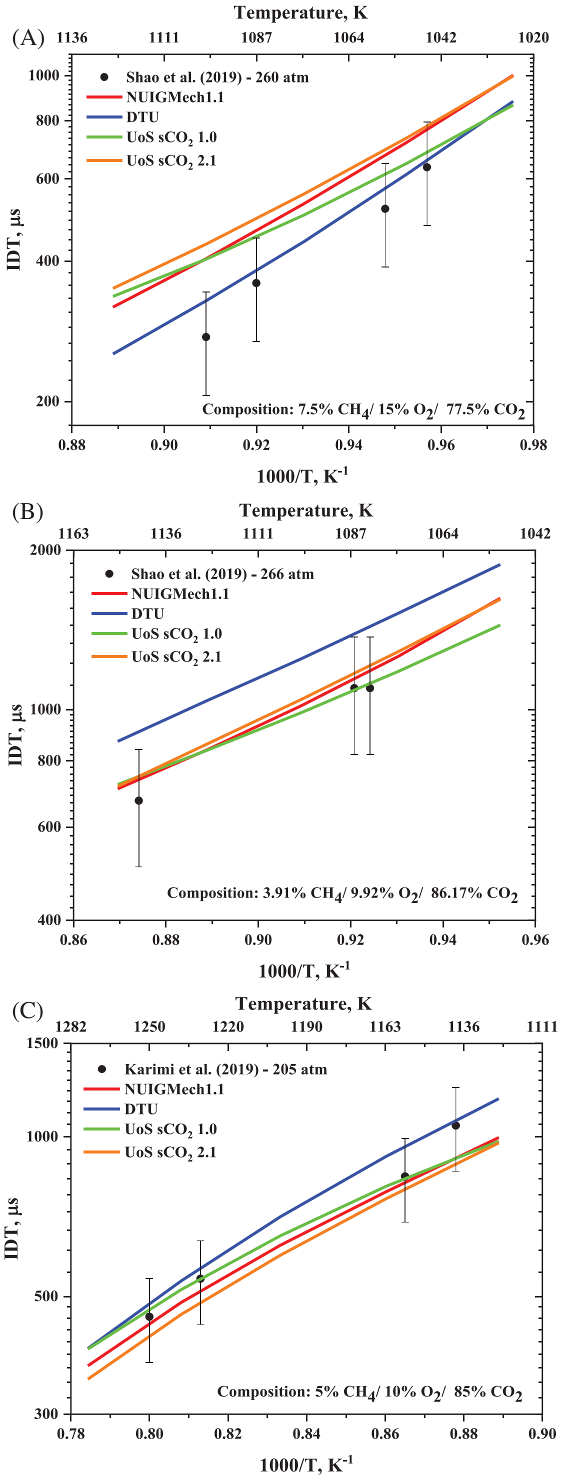

FIGURE 11 Comparison of four chemical kinetic mechanisms to IDT data from Shao et al.[20] and Karimi et al.[12]

beyond those for which they were validated is no longer adequate.

Additionally, the development of new rate coefficients which deviate from that which is currently accepted must be carefully considered, regarding their validity and effect on the overall chemistry of combustion. For example, Xu et al.[51] recently determined a rate coefficient of hydrogen abstraction of methane by CH_3O_2 (Reaction 2) which is over 100 times faster than that currently used in UoS sCO_2 2.0[33,34] above 1000 K. This would significantly increase the impact of Reaction 2 on CH_3O_2 formation from the 2.3% shown in Figure 2. However, as UoS sCO_2 2.0 is looking at modeling combustion a specific environment of large CO_2 dilutions and high-pressures, each new rate coefficient must be carefully evaluated based on its influence on the mechanisms ability to simulate experimentally determined combustion characteristics such as IDT.

The two most important rate coefficients for reinvestigation are Reactions 6 and 8 as identified by the RPA. Reaction 8 is responsible for 50% of CH_3O_2 consumption and over 30% of CH_3O formation at 1000 K (see Figure 4). The rate coefficient used in all of the mechanisms investigated in Section 7 is from a 1988 publication by Keiffer et al.[27] This work utilized a laser photolysis technique to study CH_3 decay curves which were subsequently fitted using a global technique to determine the rate coefficient of Reaction 1 and Reaction 8 at 1 atm over a narrow temperature range (293-530 K). Due to the importance of this reaction, it should be investigated as a priority for future research into the development of a mechanism for modelling high-pressure methane mechanism. Similarly, Reaction 6 was last studied by Lightfoot et al.[23] in 1991 between 600 and 719 K at atmospheric in flash photolysis study and RRKM calculations. Studying these two reactions under high-pressure conditions using modern experimental and theoretical techniques over a much broader temperature range is the next research hurdle to properly understanding the high-pressure reaction pathway of CH_3O_2.

8.2 | Ignition delay time studies

Furthermore, more experimental IDT data is required for the combustion of methane at pressures between 50 and 300 bar in CO_2, N_2, and Ar to ratify the currently accepted CH_3O_2 chemistry in terms of mechanism performance in these conditions. This would add important data for further mechanism refinement of the CH_3O_2 chemistry and is essential to justifying some of the rate coefficients used in current mechanisms which are based on estimates or limited experimental and theoretical data. This is essential to allow accurate modeling of combustion in the Allam-Fetvedt cycle and therefore used to increase performance and efficiency. Most shock tube facilities can only operate at pressures below 100 bar due to safety constraints in having sufficient design pressure to withstand detonation. This limits the potential to attain more methane IDT datasets under conditions where the chemistry of CH_3O_2 is relevant, as the temperature must also be below 1200 K, which means longer test times are required. This can be achieved by studying methane ignition in rapid compression machines.

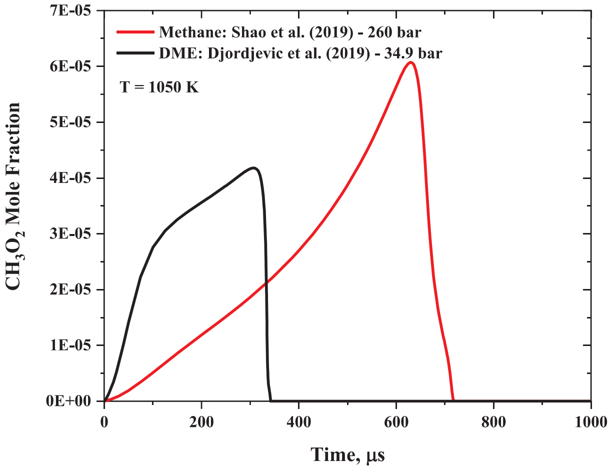

FIGURE 12 CH_3O_2 mole fraction for DME mixture (6.4% DME/19.2% O_2/74.4% CO_2) at 34.9 bar from Djordjevic et al.[55] and methane mixture (7.5% CH_4/15% O_2/77.5% CO_2) at 260 bar from Shao et al.[20] simulated by NUIGMech1.1.

It is possible to validate the rate coefficients of CH_3O_2 using different fuels with form CH_3O_2 at lower pressures and with short ignitions at lower temperatures. The two obvious candidates are dimethyl ether (DME) and diethyl ether (DEE). Chemkin simulations (see Figure 12) using the NUIGMech1.1[52–54] chemical kinetic mechanism shows that the maximum mole fraction of CH_3O_2 from a 38.4 atm (6.4% DME/19.2% O_2/74.4% CO_2) mixture at 900 K from Djordjevic et al.[55] is the same as that produced from methane ignition at 260 atm (75% CH_4/15% O_2/77.5% CO_2) from Shao et al.[20] at 1050 K. NUIGMech1.1 was used as UoS sCO_2 2.1 does not contain any DME chemistry. Furthermore, Issayev et al.[56] found that CH_3O_2 played an important role in the ignition of DEE and DEE/ethanol blends over temperature and pressure ranges of 500–1000 K and 20–40 bar, respectively. Thus, the rate coefficients of the key reactions discussed in this work can be further validated using the DME and DEE experimental data.

9 | CONCLUSION

This work takes this further by investigating the importance of CH_3O_2 chemistry to high-pressure combustion in CO_2. Identifying its importance to methane combustion above 50 bar at temperatures below 1200 K, where the absence of CH_3O_2 chemistry can lead to an increase in the IDT by up to 140%. As CH_3O_2 is formed in its entirety through the recombination of CH_3 and O_2, the branching ratio compared to Reaction 33 is essential. It has been demonstrated that at 1 bar, CH_3O_2 formation is negligible, but becomes the dominant CH_3O_2 branching pathway at points during the reaction at 300 bar. Furthermore, the UoS sCO_2 2.1 mechanism was created by updating the reactions of CH_3O_2 to the most up-to-date rate coefficients as shown in Table 1. It was identified that Reaction 6 ($CH_3O_2 + CH_3 = CH_3O + CH_3O$) and Reaction 8 ($CH_3O_2 + HO_2 = CH_3O_2H + OH$) are essential to high-pressure methane combustion and are a priority to restudy using experimental and theoretical techniques. Furthermore, it was noted that the selection of rate coefficient for Reaction 5 had a large impact on the importance of the methanol reaction pathway and thus this reaction should be studied at pressures relevant to the Allam-Fetvedt cycle. It was identified that DME and DEE produced similar maximum mole fractions of CH_3O_2 at lower pressures and temperatures than methane, which are more achievable in experimental studies. Therefore, the chemistry of DME and DEE should be added to UoS sCO_2 2.1 and validated using existing IDT data to further validate the mechanism. Furthermore, rapid compression machines should be used to generate methane ignition data at lower temperatures due to the longer test times achievable.

ACKNOWLEDGEMENTS

The work of UoS was supported by EPSRC Centre for Doctoral Training in Resilient Decarbonised Fuel Energy Systems (Grant number: EP/S022996/1) and the International Flame Research Federation (IFRF).

DATA AVAILABILITY STATEMENT

None.

ORCID

James M. Harman-Thomas https://orcid.org/0000-0003-3287-6050

REFERENCES

1. Oxford A. Ukraine war threatens European climate goals. Emerald Expert Briefings. 2022. no. oxan-db.
2. Liadze I, Macchiarelli C, Sanchez Juanino P, Mortimer-Lee P. The economic costs of the Russia-Ukraine conflict.NIESR Policy Paper, No.32. 2022. https://www.niesr.ac.uk/publications/economic-costs-russia-ukraine-conflict?type=policy-papers
3. Watson R, McCarthy J, Canziani P, Nakicenovic N, Hisas L. *The truth behind the climate pledges*. FEU-US; 2019.
4. Allam RJ, Palmer MR, Brown GW, et al. High efficiency and low cost of electricity generation from fossil fuels while eliminating atmospheric emissions, including carbon dioxide. *Energy Procedia*. 2013;37:1135-1149. doi:10.1016/j.egypro.2013.05.211
5. Lariviere B, Marion J, Macadam S, et al. "sCO_2 power cycle development and step demo pilot project". 4th European sCO_2 Conference for Energy Systems: March 23-24, 2021, Online Conference, 2021:352-362.
6. Rathi A. U.S. startup plans to build first zero-emission gas power plants. Bloomberg Green. Accessed April 15, 2021. https://www.bloomberg.com/news/articles/2021-04-15/u-s-startup-plans-to-build-first-zero-emission-gas-power-plants
7. Kelsall G. 8 Rivers Capital and Sembcorp Energy UK's first zero emissions power plant. IFRF. Accessed August 2, 2021. https://ifrf.net/ifrf-blog/8-rivers-capital-and-sembcorp-energy-uk-to-develop-uks-first-net-zero-emissions-power-plant/
8. Coogan S, Gao X, McClung A, Sun W. Evaluation of kinetic mechanisms for direct fired supercritical oxy-combustion of natural gas. Presented at the Conference: ASME Turbo Expo 2016: Turbo-machinery Technical Conference and Exposition, Seoul, South Korea; 2016. [Online]. Available: doi:10.1115/GT2016-56658
9. Harman-Thomas JM, Hughes KJ, Pourkashanian M. The development of a chemical kinetic mechanism for combustion in supercritical carbon dioxide. *Energy*. 2022:255:124490. doi:10.1016/j.energy.2022.124490
10. Harman-Thomas JM, Kashif TA, Hughes KJ, Pourkashanian M, Farooq A. Experimental and modelling study of hydrogen ignition in CO2 bath gas. *Fuel*. 2023;334:126664. doi:10.1016/j.fuel.2022.126664
11. Harman-Thomas JM, Kashif TA, Hughes KJ, Pourkashanian M, Farooq A. Experimental and modelling study of syngas combustion in CO2 bath gas. *Fuel*. 2023;342:127865. doi:10.1016/j.fuel.2023.127865
12. Karimi M, Ochs B, Liu Z, Ranjan D, Sun W. Measurement of methane autoignition delays in carbon dioxide and argon diluents at high pressure conditions. *Combust Flame*. 2019;204:304-319. doi:10.1016/j.combustflame.2019.03.020
13. Assaf E, Sheps L, Whalley L, et al. The reaction between CH_3O_2 and OH radicals: product yields and atmospheric implications. *Environ Sci Technol*. 2017;51(4):2170-2177. doi:10.1021/acs.est.6b06265
14. Fittschen C, Whalley LK, Heard DE. The reaction of CH_3O_2 radicals with OH radicals: a neglected sink for CH_3O_2 in the remote atmosphere. *Environ Sci Technol*. 2014;48(14):7700-7701. doi:10.1021/es502481q
15. Villenave E, Lesclaux R. Kinetics of the cross reactions of CH_3O_2 and $C_2H_5O_2$ radicals with selected peroxy radicals. *J Phys Chem*. 1996;100(34):14372-14382. doi:10.1021/jp960765m
16. Jafri JA, Phillips DH. Ground and lower excited states of methylperoxy radical, CH_3O_2: a computational investigation. *J Am Chem Soc*. 1990;112(7):2586-2590. doi:10.1021/ja00163a017
17. Hashemi H, Christensen JM, Gersen S, Levinsky H, Klippenstein SJ, Glarborg P. High-pressure oxidation of methane. *Combust Flame*. 2016;172:349-364. doi:10.1016/j.combustflame.2016.07.016

18. Wang H, You X, Joshi AV, et al. High-temperature combustion reaction model of H_2. High-temperature Combustion Reaction Model of H_2/CO/C1-C4 Compounds. 2007.
19. Smith GP, Golden DM, Frenklach M, et al. GRI Mechanism 3.0. University of California, Berkeley. Accessed December 16, 2019. http://combustion.berkeley.edu/gri-mech/version30/text30.html
20. Shao J, Choudhary R, Davidson DF, Hanson RK, Barak S, Vasu S. Ignition delay times of methane and hydrogen highly diluted in carbon dioxide at high pressures up to 300 atm. *Proc Combust Inst*. 2019;37(4):4555-4562. doi:10.1016/j.proci.2018.08.002
21. Smith GP, Tao Y, Wang H. Foundational Fuel Chemistry Model Version 1.0 (FFCM-1), http://nanoenergy.stanford.edu/ffcm1, 2016.
22. Wang Z, Zhao H, Yan C, et al. Methanol oxidation up to 100 atm in a supercritical pressure jet-stirred reactor. *Proceedings of the Combustion Institute*, 2022. doi:10.1016/j.proci.2022.07.068
23. Lightfoot PD, Roussel P, Caralp FO, Lesclaux R. Flash-photolysis study of the CH_3O_2 + CH_3O_2 and CH_3O_2 + HO_2 reactions between 600 and 719 K – unimolecular decomposition of methylhydroperoxide. *J Chem Soc, Faraday Trans*. 1991;87(19):3213-3220. doi:10.1039/ft9918703213
24. Bossolasco A, Faragó EP, Schoemaecker C, Fittschen C. Rate constant of the reaction between CH_3O_2 and OH radicals. *Chem Phys Lett*. 2014;593:7-13. doi:10.1016/j.cplett.2013.12.052
25. Lightfoot PD, Roussel P, Caralp FO, Lesclaux R. Flash-photolysis study of the CH_3O_2 + CH_3O_2 and CH_3O_2 + HO_2 reactions between 60 and 719 K – Unimolecular decomposition of methylhydroperoxide. *J Chem Soc, Faraday Trans*. 1991;87(19):3213-3220. doi:10.1039/ft9918703213
26. Rasmussen CL, Wassard KH, Dam-Johansen K, Glarborg P. Methanol oxidation in a flow reactor: implications for the branching ratio of the CH_3OH+OH reaction. *Int J Chem Kinet*. 2008;40(7):423-441. doi:10.1002/kin.20323
27. Keiffer M, Miscampbell AJ, Pilling MJ. A global technique for analysing multiple decay curves. Application to the CH_3 + O_2 system. *J Chem Soc, Faraday Trans 2*. 1988;84(5):505-514.
28. Baulch DL, Bowman CT, Cobos CJ, et al. Evaluated kinetic data for combustion modeling: supplement II. *J Phys Chem Ref Data*. 2005;34(3):757-1397. doi:10.1063/1.1748524
29. Tsang W, Hampson RF. Chemical kinetic data base for combustion chemistry. Part I. Methane and related compounds. *J Phys Chem Ref Data*. 1986;15(3):1087-1279. doi:10.1063/1.555759
30. Labbe NJ, Sivaramakrishnan R, Goldsmith CF, Georgievskii Y, Miller JA, Klippenstein SJ. Weakly bound free radicals in combustion: "Prompt" dissociation of formyl radicals and its effect on laminar flame speeds. *J Phys Chem Lett*. 2016;7(1):85-89. doi:10.1021/acs.jpclett.5b02418
31. Jasper AW, Klippenstein SJ, Harding LB. Theoretical rate coefficients for the reaction of methyl radical with hydroperoxyl radical and for methylhydroperoxide decomposition. *Proc Combust Inst*. 2009;32(1):279-286. doi:10.1016/j.proci.2008.05.036
32. Carstensen H-H, Dean AM, Deutschmann O. Rate constants for the H abstraction from alkanes (R–H) by R′O2 radicals: a systematic study on the impact of R and R′. *Proc Combust Inst*. 2007;31(1):149-157. doi:10.1016/j.proci.2006.08.091
33. Wu Y, Panigrahy S, Sahu AB, et al. Understanding the antagonistic effect of methanol as a component in surrogate fuel models: a case study of methanol/n-heptane mixtures. *Combust Flame*. 2021;226:229-242.
34. Baigmohammadi M, Patel V, Nagaraja S, et al. Comprehensive experimental and simulation study of the ignition delay time characteristics of binary blended methane, ethane, and ethylene over a wide range of temperature, pressure, equivalence ratio, and dilution. *Energy Fuels*. 2020;34(7):8808-8823. doi:10.1021/acs.energyfuels.0c00960
35. Sander SP, Watson RT. Kinetics studies of the reactions of CH_3O_2 with NO, NO_2, and CH_3O_2 at 298 K. *J Phys Chem*. 1980;84(13):1664-1674.
36. Bogdanchikov GA, Baklanov AV, Parker DH. The substitution reactions $RH+O_2 \rightarrow RO_2+H$: transition state theory calculations based on the ab initio and DFT potential energy surface. *Chem Phys Lett*. 2004;385(5):486-490. doi:10.1016/j.cplett.2004.01.015
37. Zhang F, Huang C. Pressure-dependent kinetics of the reaction between CH_3OO and OH focusing on the product yield of methyltrioxide (CH_3OOOH). *J Phys Chem Lett*. 2019;10(13):3598-3603. doi:10.1021/acs.jpclett.9b00781
38. Elrod MJ, Ranschaert DL, Schneider NJ. Direct kinetics study of the temperature dependence of the CH_2O branching channel for the CH_3O_2 + HO_2 reaction. *Int J Chem Kinet*. 2001;33(6):363-376. doi:10.1002/kin.1030
39. Zhao Z, Song J, Su B, Wang X, Li Z. Mechanistic study of the reactions of methyl peroxy radical with methanol or hydroxyl methyl radical. *J Phys Chem A*. 2018;122(23):5078-5088. doi:10.1021/acs.jpca.7b09988
40. Slemr F, Warneck P. Kinetics of the reaction of atomic hydrogen with methyl hydroperoxide. *Int J Chem Kinet*. 1977;9(2):267-282. doi:10.1002/kin.550090210
41. Ing W-C, Sheng CY, Bozzelli JW. Development of a detailed high-pressure reaction model for methane/methanol mixtures under pyrolytic and oxidative conditions and comparison with experimental data. *Fuel Process Technol*. 2003;83(1):111-145. doi:10.1016/S0378-3820(03)00062-6
42. Allam RJ, Fetvedt JE, Forrest BA, Freed DA. The oxy-fuel, supercritical CO_2 Allam cycle: new cycle developments to produce even lower-cost electricity from fossil fuels without atmospheric emissions. *Proceedings of the Asme Turbo Expo: Turbine Technical Conference and Exposition*. 3b, 2014, Art no. V03bt36a016.
43. Yan C, Kocevska S, Krasnoperov LN. Kinetics of the reaction of CH_3O_2 radicals with OH studied over the 292–526 K temperature range. *J Phys Chem A*. 2016;120(31):6111-6121.
44. Huang J, Hill PG, Bushe WK, Munshi SR. Shock-tube study of methane ignition under engine-relevant conditions: experiments and modeling. *Combust Flame*. 2004;136(1):25-42. doi:10.1016/j.combustflame.2003.09.002
45. Petersen E, Davidson D, Hanson R. Kinetics modeling of shock-induced ignition in low-dilution CH_4/O_2 mixtures at high pressures and intermediate temperatures. *Combust Flame*. 1999;117(1):272-290. doi:10.1016/S0010-2180(98)00111-4
46. O'Callaghan J. The wild physics of Elon Musk's methane-guzzling super-rocket. Wired. Accessed February 11, 2021. https://www.wired.co.uk/article/spacex-raptor-engine-starship
47. Hargis JW, Petersen EL. Methane ignition in a shock tube with high levels of CO_2 dilution: consideration of the reflected-shock bifurcation. *Energy Fuels*. 2015;29(11):7712-7726. doi:10.1021/acs.energyfuels.5b01760

48. Hashemi H, Christensen JM, Glarborg P. High-pressure pyrolysis and oxidation of DME and DME/CH_4. *Combust Flame*. 2019;205:80-92. doi:10.1016/j.combustflame.2019.03.028
49. Yan C, Krasnoperov LN. Pressure-dependent kinetics of the reaction between CH_3O_2 and OH: TRIOX formation. *J Phys Chem A*. 2019;123(39):8349-8357. doi:10.1021/acs.jpca.9b03861
50. Fernandes RX, Luther K, Troe J. Falloff curves for the reaction $CH_3 + O_2$ (+M) → CH_3O_2 (+M) in the pressure range 2−1000 bar and the temperature range 300−700 K. *J Phys Chem A*. 2006;110(13):4442-4449. doi:10.1021/jp056850o
51. Xu S, Liang J, Cao S, He R, Yin G, Wang Q-D. A hierarchical theoretical study of the hydrogen abstraction reactions of H2/C1–C4 molecules by the methyl peroxy radical and implications for kinetic modeling. *ACS Omega*. 2022;7(10):8675-8685. doi:10.1021/acsomega.1c06683
52. Metcalfe WK, Burke SM, Ahmed SS, Curran HJ. A hierarchical and comparative kinetic modeling study of C1 − C2 hydrocarbon and oxygenated fuels. *Int J Chem Kinet*. 2013;45(10):638-675. doi:10.1002/kin.20802
53. Burke U, Metcalfe WK, Burke SM, Heufer KA, Dagaut P, Curran HJ. A detailed chemical kinetic modeling, ignition delay time and jet-stirred reactor study of methanol oxidation. *Combust Flame*. 2016;165:125-136. doi:10.1016/j.combustflame.2015.11.004
54. Kéromnès A, Metcalfe WK, Heufer KA, et al. An experimental and detailed chemical kinetic modeling study of hydrogen and syngas mixture oxidation at elevated pressures. *Combust Flame*. 2013;160(6):995-1011. doi:10.1016/j.combustflame.2013.01.001
55. Djordjevic N, Rekus M, Vinkeloe J, Zander L. Shock tube and kinetic study on the effects of CO_2 on dimethyl ether autoignition at high pressures. *Energy Fuels*. 2019;33(10):10197-10208. doi:10.1021/acs.energyfuels.9b01575
56. Issayev G, Mani Sarathy S, Farooq A. Autoignition of diethyl ether and a diethyl ether/ethanol blend. *Fuel*. 2020;279:118553. doi:10.1016/j.fuel.2020.118553

How to cite this article: Harman-Thomas JM, Ingham DB, Hughes KJ, Pourkashanian M. Role of methyldioxy radical chemistry in high-pressure methane combustion in CO_2. *Int J Chem Kinet*. 2023;1-13. https://doi.org/10.1002/kin.21672